Materials Science and Engineering B 109 (2004) 24–29

www.elsevier.com/locate/mseb

Pulsed laser deposition of thin Pr_xO_y films on Si(1 0 0)

D. Wolfframm [a,*], M. Ratzke [a], M. Kappa [a], M.J. Montenegro [b], M. Döbeli [b], Th. Lippert [b], J. Reif [a]

[a] *IHP/BTU JointLab, and BTU Cottbus, LS Experimentalphysik II, Universitätsplatz 3-4, 03044 Cottbus, Germany*
[b] *Paul Scherrer Institut, 5232 Villigen, Switzerland*

Abstract

Pr_xO_y thin films have been grown by pulsed laser deposition (PLD) on Si(1 0 0) surfaces. The chemical composition of layers with different thickness was investigated using core level (Pr 3d, O 1s, Si 2p) X-ray photoelectron emission spectroscopy (XPS). The line shape analysis of emission spectra does not indicate any interfacial mixing but suggests the formation of a silicate (Si–O–Pr) at the Pr_xO_y/Si interface. Although Pr_6O_{11} was used as target material, XPS spectra have shown that the Pr_xO_y films consist of two Pr-oxides (Pr_2O_3, Pr_6O_{11}). The intensity ratio of the two Pr-oxides did not change with increasing film thickness but the Pr and O core levels are slightly shifted toward lower binding energy. Using Rutherford backscattering spectroscopy (RBS) we found a much too high O/Pr intensity ratio for Pr_xO_y layers grown at room temperature. For layers grown at 650 °C the ratio was within the expected range.

Keywords: High-k gate dielectric material; Praseodymium oxide; Pulsed laser deposition

1. Introduction

The International Roadmap for Semiconductors [1] predicts that the minimum feature size of CMOS devices will shrink to about 70 nm by the year 2009. Assuming that SiO_2 would still be dielectric material of choice, then its films thickness has to be reduced down to less than 1 nm to obtain a high enough gate capacitance. Already well before the fundamental physical limit of ∼0.7 nm [2–4] is reached, the gate leakage current density increases dramatically with decreasing oxide thickness (up to 10 A/cm^2 at 1.5 nm [5–7]). In order to overcome this problem, an alternative material with higher dielectric constant has to be found.

Although many different high-k materials have been researched so far (e.g., hafnium oxide, etc. [8]), the ideal replacement for SiO_2 has not been found yet, a number of difficulties such as interface reaction and leakage current density value still existing. One potential candidate, the high-k material praseodymium oxide, should exhibit a dielectric constant almost 10 times higher than SiO_2 ($k_{SiO2} = 3.9$). While the Pr_2O_3 configuration has been studied comprehensively [9–12], our investigation is focussed on Pr_6O_{11}, which would represent the highest k-value of the Pr-oxides.

To preserve the stoichiometric ratio of the source material (Pr_6O_{11}) in the fabricated films we use pulsed laser deposition (PLD). This advantage of PLD was proved earlier for the growth of high-T_C superconductor films [13]. In an earlier report [14], we published already experimental results, investigating the influence of growth parameters as well as laser parameters on the praseodymium oxide surface morphology and on the interface properties.

Here, we concentrate on the chemical composition of the grown praseodymium oxide layers investigated by means of X-ray photoelectron emission spectroscopy (XPS). Rutherford backscattering (RBS) measurements support the XPS results about the chemical layer composition.

2. Experimental

All PLD experiments were carried out in a two-chamber UHV-system (Fig. 1). The base pressure was in the lower 10^{-10} mbar range (during the PLD process: ∼10^{-7} mbar). As substrates we used 12 mm × 8 mm pieces cleaved from p-Si (100 ± 0.25°) wafers (1–20 Ω cm). After an ex situ chemical cleaning and an in situ thermal processing the LEED pattern showed the well known (2 × 1)/(1 × 2) su-

* Corresponding author. Tel.: +49-355-69-3185; fax: +49-355-69-3985.
E-mail address: dirk.wolfframm@tu-cottbus.de (D. Wolfframm).

0921-5107/$ – see front matter © 2003 Published by Elsevier B.V.
doi:10.1016/j.mseb.2003.10.022

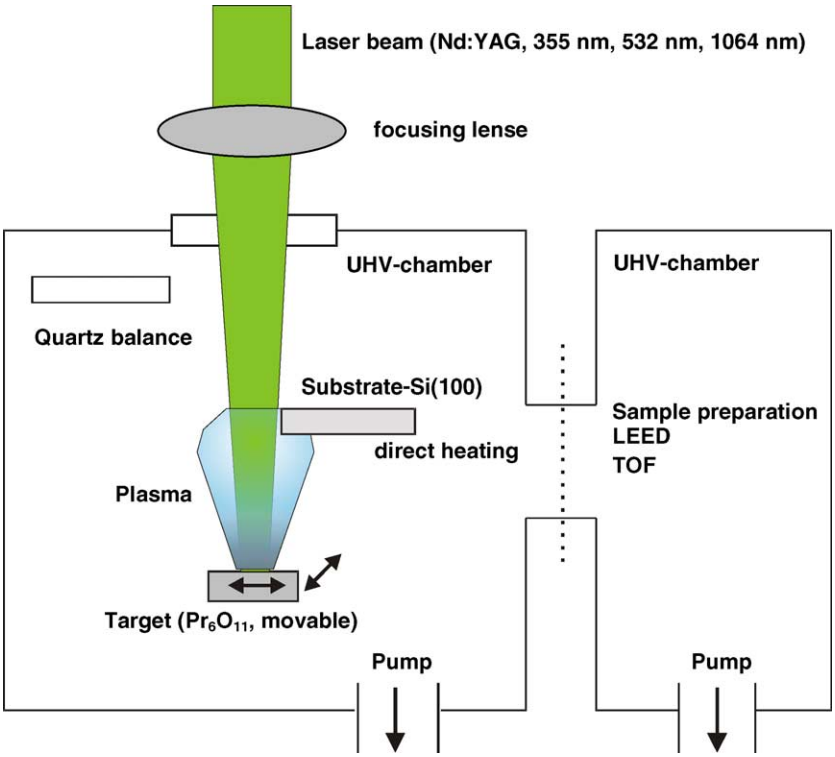

Fig. 1. A schematic diagram of the experimental arrangement for the growth of thin Pr_xO_y films on p-Si(1 0 0) substrates by pulsed laser deposition. The Pr_6O_{11} target material was placed in a Ta-holder which was moved continuously during the whole growth procedure.

perstructure as an evidence for a clean and well ordered Si(1 0 0) surface [14].

For the ablation from the sintered Pr_6O_{11} targets (purity 99.9%) a pulsed Nd:YAG laser (wavelength: 355 nm; pulse duration: 10 ns; fluence: 1 J/cm^2) was used. The target was placed in a tantalum box, which was scanned continuously during the PLD procedure (Pr_xO_y growth rate: 8–40 Å/min; substrate temperature: varied from room temperature (RT) up to 900 °C).

After growth the samples were transferred to a separate chamber equipped with a commercial XPS-spectrometer. Al K_α ($h\nu = 1486.6$ eV) excited core level spectra (Pr $3d_{5/2}$, O 1s, and Si 2p) were processed using a non-linear least square fitting procedure. RBS, with less surface sensitivity than XPS, was used to analyse the chemical composition and the crystal structure quality.

3. Results and discussion

3.1. XPS investigation

Unfortunately, the known XPS data for Pr_2O_3 and PrO_2 [15–19] are not too reliable. However, regarding the crystal field and the crystal structure, the positions of the Pr_6O_{11} target core levels should be between those of Pr_2O_3 and PrO_2 closer to PrO_2 due to the similar chemical composition. In order to determine absolute core level positions, charging effects have to be considered, in particular when analysing data from praseodymium oxide target material and thick layers, respectively.

3.1.1. Pr 3d–XPS spectra

Fig. 2 shows a set of Pr $3d_{5/2}$ spectra taken for the Pr_6O_{11} target material (lower trace) and two samples of different praseodymium oxide thickness as illustrated. Both layers were grown at 650 °C.

3.1.1.1. Pr_6O_{11} target. The expected line shape of the Pr $3d_{5/2}$ spectra is clearly visible, with two maxima, separated by 4.4 eV binding energy [15]. The detailed shape of the signal can only be fitted assuming the contribution of 4 components, belonging in pairs to two different chemical environments. This means that the target material already consists of two Pr-oxides, Pr_6O_{11} and, most likely, Pr_2O_3.

Two reasons could be responsible for this discrepancy with the nominal target composition: (a) the thermal instability of the Pr_6O_{11} could cause the chemical transformation. It is known that Pr_6O_{11} changes to a composition with less oxygen at temperatures higher than 480 °C. This temperature may be reached during the target sinter process and especially in the laser induced plasma plume at the target. (b) The Pr_6O_{11} target material easily reacts with water and forms praseodymium hydroxide [$Pr(OH)_3$] accompanied by the formation of PrO_2 [18].

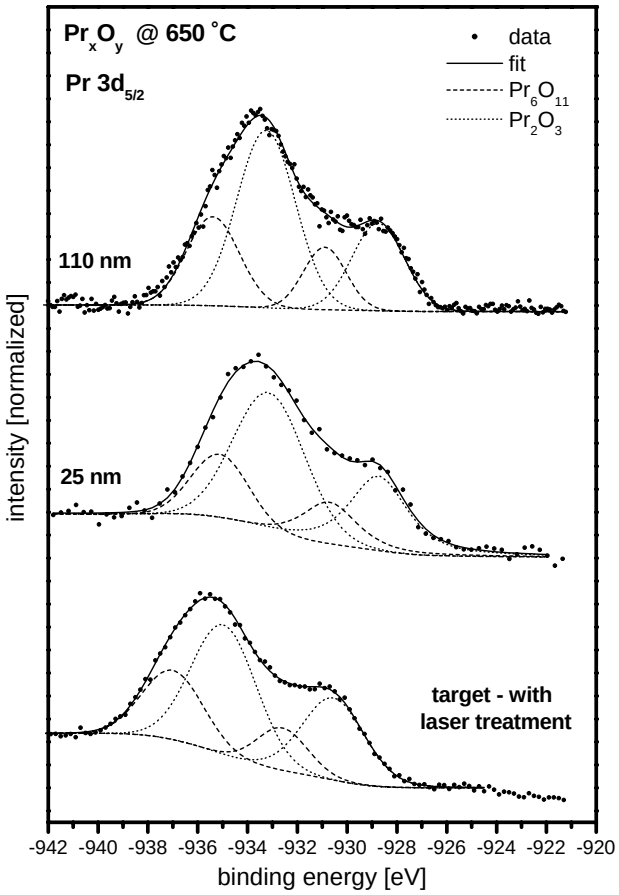

Fig. 2. Set of Pr $3d_{5/2}$ XPS spectra for the Pr_6O_{11} target material, and for various Pr_xO_y layer thickness as indicated. The different components needed to fit the spectra are labelled. Two fit components are attributed to Pr_2O_3 and to Pr_6O_{11}, respectively. The Pr-oxide intensity ratio $Pr^{+4}(Pr_6O_{11})$:$Pr^{+3}(Pr_2O_3) = 1{:}2$ does not change significantly with increasing layer thickness.

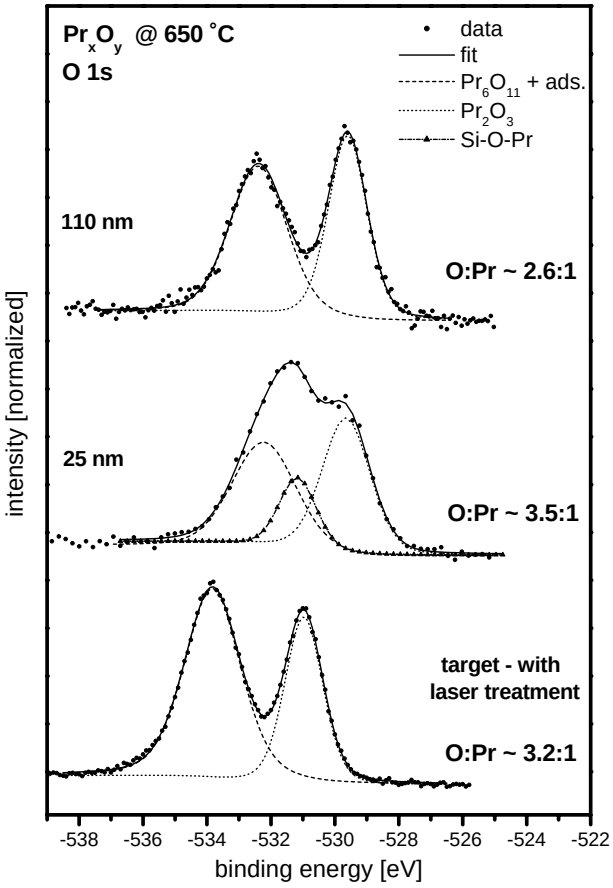

Fig. 3. XPS spectra of the O 1s state for the Pr_6O_{11} target material, and for various Pr_xO_y layer thickness as indicated. For each spectrum one fit component is attributed to Pr_2O_3 and another to Pr_6O_{11}. Between the two Pr-oxides an additional component arises at 25 nm layer thickness, which is attributed to a silicate-like Si–O–Pr configuration. At 110 nm layer thickness the total oxygen to praseodymium intensity ratio approaches its minimum (2.6:1).

In fact, from these species we should observe two different charge states of the Pr-ion: Pr^{+3} in Pr_2O_3 and $Pr(OH)_3$ and Pr^{+4} in Pr_6O_{11} and PrO_2. Though it is difficult to unambiguously attribute the signals, we associate the line pair at higher binding energies (∼937, ∼933 eV) to Pr^{+4} and that at lower binding energies (∼935, ∼931 eV) to Pr^{+3}. Obviously, the Pr^{+3} signal is almost twice as large as the Pr^{+4} signal.

3.1.1.2. Pr_xO_y layers. For the Pr_xO_y films, the spectra are slightly shifted to lower binding energies as compared to the target, in particular during the initial stages of growth.

The corresponding Pr $3d_{5/2}$ spectra of samples with different Pr_xO_y layer thickness, 25 and 110 nm, respectively, are shown in Fig. 2 (middle and upper graph). Still, 4 components are needed for a sufficient fitting, two for the components at higher binding energy (935.3, 930.8 eV: Pr_6O_{11}), and two for the components at lower binding energy (933.2 and 928.7 eV: Pr_2O_3). However, neither the line shape nor the intensity ratio (Pr^{+4}:Pr^{+3} = 1:2) differ significantly from those of the target.

To estimate the total film O/Pr-ratio, we used the Pr 3d components. The O/Pr-ratio for Pr_2O_3 (Pr^{+3}) is 1.5 and for Pr_6O_{11} (Pr^{+4}) is 1.8. Taking into account the observation of $Pr^{+3}/Pr^{+4} = 2/1$, we can derive the layer O/Pr-ratio: ∼1.6.

3.1.2. O 1s–XPS spectra

In order to obtain a comprehensive impression about the Pr_xO_y layer stoichiometry the O 1s signal was also investigated (Fig. 3).

3.1.2.1. Pr_6O_{11} target. One component (∼534.5 eV) attributed to Pr_6O_{11} and another component (∼531.5 eV) attributed to Pr_2O_3 are necessary to fit the O 1s spectrum of the target (see Fig. 3, bottom spectrum) indicating the presence of two Pr-oxides. Neglecting the splitting into different chemical environment and considering the different atomic sensitivity factors, the element ratio O to Pr can be calculated to 3.2:1. This value is too high for the pure oxides, suggesting a ratio <2:1. The strong hygroscopic behaviour could explain this extremely high oxygen intensity. Lütke-

hoff et al. [18] investigated the hydroxide formation upon the dissociation of water and attributed an O 1s signal at 532 eV to Pr-hydroxide. Most likely, the oxygen contained in adsorbates will also influence the high O 1s intensity. The O 1s component caused by adsorbates should overlap the O 1s component from Pr_6O_{11}. Therefore, we suggest that the O 1s component at 534.5 eV is a mixture of both.

3.1.2.2. Pr_xO_y layers. In comparison with the target O 1s spectrum, the spectrum from a sample with 25 nm Pr_xO_y layer thickness is changed significantly, as shown in Fig. 3 (middle). There are still two main components at 532.2 and 529.6 eV binding energy, which are attributed to oxygen in Pr_6O_{11} and Pr_2O_3, respectively. Due to the growth temperature of 650 °C the Pr-hydroxide formation is very unlikely. The peak at 529.6 eV is caused only by Pr_2O_3 [17]. However, to fit this spectrum an additional component at 531.1 eV has to be taken into account. Investigating the surface morphology reveals that the Pr_xO_y layer does not grow homogeneously, resulting in a not perfectly closed film. Consequently, interface information can be recorded even at this relatively thick layer (25 nm). Assuming SiO_2-formation at the interface would result in a peak at higher binding energy of 532.7 eV [20] and can, therefore, be excluded. However, it is known that rare-earth oxides easily react with Si to form silicate-like Si–O–metal configurations [8,21]. Consequently, we attribute the 531.1 eV signal to oxygen in a silicate-like Si–O–Pr configuration.

At higher Pr_xO_y layer thickness (110 nm), as shown in Fig. 3 (upper spectrum), the additional component disappears and the line shape looks similar to that of the target material. Only, the intensity of the component at higher binding energy is decreased. This can be caused by a different amount of the oxygen-adsorbates contribution overlapping the Pr_6O_{11} signal. Consequently, the element ratio O/Pr is disproportionately high.

3.1.3. Si 2p–XPS spectra–Pr_xO_y layer (25 nm)

The Si 2p signal representing the interface properties is shown in Fig. 4. Clearly visible is the main peak with the maximum intensity at 99.5 eV, which belongs to the bulk signal of the Si substrate [22]. Further peaks appear at 100.5 and 101.6 eV, respectively. They can be attributed to Si-C and Si-oxide which are known to be formed during the sample preparation [23,24]. But the additional component at 102.7 eV cannot be attributed to SiO_2, which would appear at 103.6 eV binding energy [25]. As suggested by Fissel et al. [17] this peak could be caused by a Si-oxide with an ionic charge of +3, and so having an interface configuration like Si–SiO_3. This implies the accumulation of oxygen at the interface caused by the high diffusion of oxygen which is a well known behaviour of rare-earth oxides. In line with this argument, we attribute the component at 102.7 eV to a silicate-like Si–O–Pr configuration, thus confirming the interpretation of a silicate being at the origin of the additional O 1s component in the spectra in Fig. 3 (middle).

3.2. RBS measurements

For an alternative analysis of the chemical layer composition two other Pr_xO_y samples were prepared and investigated by RBS. The Pr_xO_y film thickness was 37 nm. One sample was grown at RT and another grown at 650 °C.

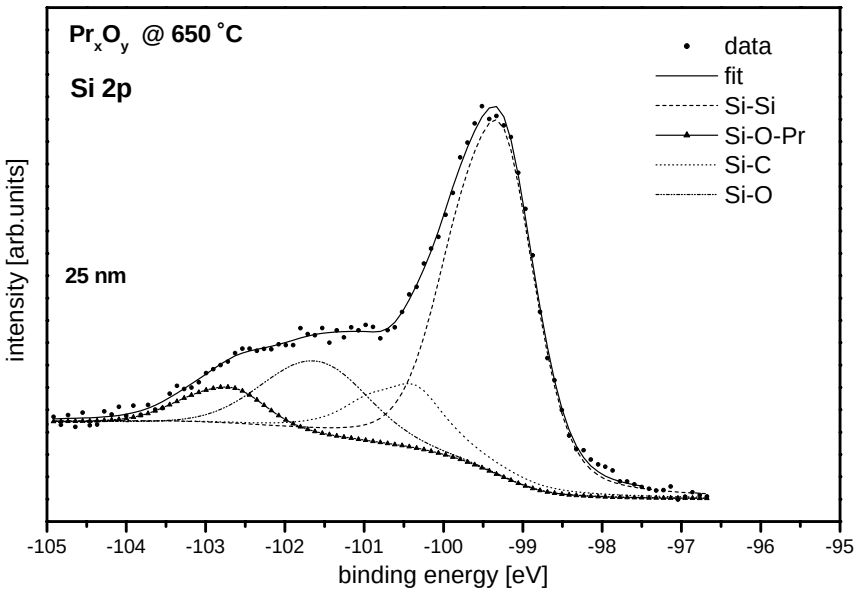

Fig. 4. Photoelectron emission spectrum showing the Si 2p core level of a 25 nm thick Pr_xO_y layer grown at 650 °C substrate temperature. An additional feature at 102.7 eV binding energy appears, caused by an accumulation of oxygen at the interface. Considering the corresponding O 1s spectrum the component can be attributed to the expected silicate-like Si–O–Pr configuration accompanied by the formation of a Si-oxide with +3 ionic charge at the interface (Si–SiO_3).

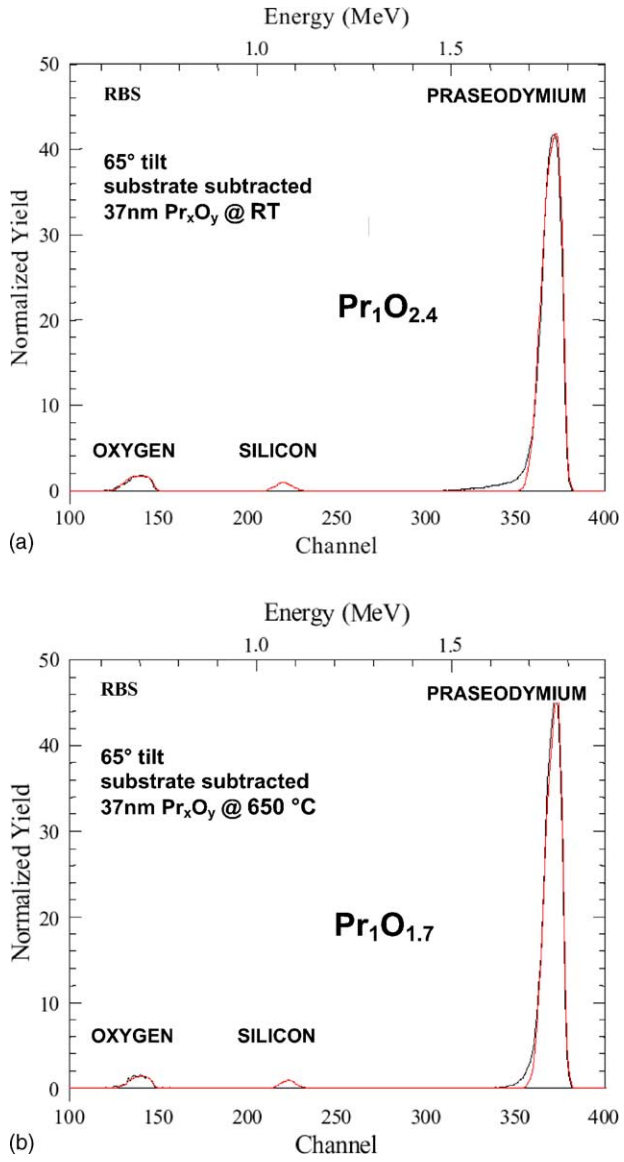

Fig. 5. The energy distribution of backscattered $^4He^+$ ions from two samples with same film thickness of 37 nm. The Pr_xO_y layers were grown at RT (upper graph) and at 650 °C (bottom graph), respectively. The peaks, corresponding to oxygen, silicon, and praseodymium are labelled. The element ratio Pr:O is indicated.

As shown in Fig. 5 (bottom graph) the intensity ratio O/Pr amounts to 1.7:1 for the layer grown at 650 °C, which is close to the intensity ratio (∼1.6) obtained by using the Pr 3d XPS data. These values agree very much with the expected value for Pr_6O_{11} of 1.8 (Pr_2O_3: 1.5).

As shown in Fig. 5 (upper graph) the element ratio O/Pr was evaluated and amounts to 2.4:1 for the layer grown at RT, i.e., the oxygen intensity is too high. This can be explained by the accumulation of water (hygroscopic behaviour) during the Pr_xO_y thin film growth.

Additional RBS channeling-Rocking curve experiments have not indicated the presence of a single crystalline Pr_xO_y film structure.

4. Conclusion

XPS and RBS studies were used to investigate the chemical composition of the Pr_xO_y/Si(1 0 0) interface and the stoichiometry of the Pr_xO_y layers. Our results indicate the existence of two Pr-oxides in the grown Pr_xO_y films. The Pr-oxide ratio in this mixture does not change with increasing film thickness.

The intensity ratio of the Pr^{+4}/Pr^{+3} components amounts to 1:2. Taking into account the Pr^{+4}/Pr^{+3} ratio, the film composition O/Pr was estimated to 1.6. RBS measurements have shown a similar value of 1.7 for Pr_xO_y films grown at 650 °C substrate temperature.

The O 1s and the Si 2p line shape analysis indicates the formation of a silicate-like Si–O–Pr configuration at the interface.

Acknowledgements

We would like to thank W. Seifert and G. Beuckert for experimental assistance and critical discussions. We gratefully acknowledge financial support by the HWP grant of the Federal Government of Germany and the State of Brandenburg.

References

[1] The International Technology Roadmap for Semiconductors, Semiconductor Industry Association, 2001, for the most recent updates see: http://public.itrs.net/.
[2] S. Tang, R.M. Wallace, A. Seabaugh, D. King-Smith, Appl. Surf. Sci. 135 (1998) 137.
[3] D.A. Muller, T. Sorsch, S. Moccio, F.H. Baumann, K. Evans-Lutterodt, G. Timp, Nature (London) 399 (1999) 758.
[4] R.R. Chau, J. Kavalieros, B. Roberds, R. Schenker, D. Lionberger, D. Barlage, B. Doyle, R. Arghavani, A. Murthy, G. Dewey, in: Proceedings of the International Electron Development Meeting, 2000, p. 45.
[5] S.M. Sze, Physics of Semiconductor Devices, second ed., Wiley, New York, 1981.
[6] B.E. Weir, P.J. Silverman, M.A. Alam, F. Baumann, D. Monroe, A. Ghetti, J.D. Bude, G.L. Timp, A. Hamad, T.M. Oberdick, in: Proceedings of the International Electron Development Meeting, 1999, p. 437.
[7] M. Buchanan, IBM J. Res. Develop. 43 (1999) 245.
[8] G.D. Wilk, R.M. Wallace, J.M. Anthony, J. Appl. Phys. 89 (2001) 5243.
[9] H.J. Müssig, J. Dabrowski, K. Ignatovich, J.P. Liu, V. Zavodinsky, H.J. Osten, Surf. Sci. 504C (2002) 159.
[10] H.J. Osten, J.P. Liu, H.J. Müssig, Appl. Phys. Lett. 80 (2002) 297.
[11] H.J. Osten, J.P. Liu, E. Bugiel, H.J. Müssig, P. Zaumseil, Mat. Sci. Eng. 87 (2001) 297.
[12] H.J. Osten, J.P. Liu, H.J. Müssig, P. Zaumseil, Microelectr. Reliability 41 (2001) 991.
[13] D. Bäuerle, Laser Processing and Chemistry, second ed., Springer, Berlin, 1996.
[14] D. Wolfframm, M. Ratzke, S. Kouteva-Arguirova, J. Reif, Mat. Sci. Semicond. Proc. 5 (2003) 429.
[15] A. Bianconi, A. Kotani, K. Okada, R. Giorgi, A. Gargano, A. Marcelli, T. Miyahara, Phys. Rev. B38 (1988) 3433.

[16] H. Ogasawara, A. Kotani, R. Potze, G.A. Sawatzky, B.T. Thole, Phys. Rev. B44 (1991) 5465.
[17] A. Fissel, J. Dabrowski, H.J. Osten, J. Appl. Phys. 91 (2002) 8986.
[18] S. Lütkehoff, M. Neumann, A. Slebarski, Phys. Rev. B52 (1995) 13808.
[19] A. Slebarski, M. Neumann, S. Mähl, Phys. Rev. B51 (1995) 11113.
[20] C.D. Wagner, D.E. Passoja, H.F. Hillery, T.G. Kinisky, H.A. Six, W.T. Jansen, J.A. Taylor, J. Vac. Sci. Technol. 21 (1982) 933.
[21] H. Ono, T. Katsumata, Appl. Phys. Lett. 78 (2001) 1832.
[22] F.G. Bell, L. Ley, Phys. Rev. B37 (1988) 8383.
[23] Y. Mizokawa, K.M. Geib, C.W. Wilmsen, J. Vac. Sci. Technol. A4 (1986) 1696.
[24] W.A.M. Aarnik, A. Weishaupt, A. van Silfout, Appl. Surf. Sci. 45 (1990) 37.
[25] J. Finster, E.-D. Klingenberg, J. Heeg, Vacuum 41 (1990) 1586.